

Quantification of southwest China rainfall during the 8.2 ka BP event with response to North Atlantic cooling

Y. Liu^{1,2}, C. Hu¹

¹ State key lab of biogeology and environmental geology, China University of Geosciences, Wuhan, 430074, PR China

² Faculty of Materials Science & Chemistry, China University of Geosciences, Wuhan, 430074, PR China

Correspondence to: Y. Liu (yhliu@cug.edu.cn)

Abstract. The 8.2 ka BP event could provide important information for predicting abrupt climate change in the future. Although published records show that the East Asian monsoon area responded to the 8.2 ka BP event, there is no high resolution quantitative reconstructed climate record in this area. In this study, a reconstructed 10-yr moving average annual rainfall record in southwest China during the 8.2 ka BP event is presented by comparing two high-resolution stalagmite $\delta^{18}\text{O}$ records from Dongge cave and Heshang cave. **This decade-scale rainfall reconstruction is based on a central-scale model and is confirmed by inter-annual monitoring records, which shows a significant positive correlation between the regional mean annual rainfall amount and the drip water annual average $\delta^{18}\text{O}$ difference from two caves along the same monsoon moisture transport pathway from May 2011 to April 2014.** Similar trends between the reconstructed rainfall and the stalagmite Mg/Ca record, another proxy of rainfall, during the 8.2 ka period further increase the confidence of the quantization of the rainfall record. The reconstructed record shows that the mean annual rainfall in southwest China during the central 8.2 ka BP event is less than that of present (1950 ~ 1990) by ~200 mm, and decreased by ~350 mm in ~70 years experiencing an extreme drying period lasting for ~50 years. Further analysis **on the reconstructed rainfall in southwest China and Greenland ice core $\delta^{18}\text{O}$ with $\delta^{15}\text{N}$ records, suggests that the rainfall decrease in southwest China during the 8.2 ka BP period coupled with Greenland cooling with a possible response rate of $110 \pm 30 \text{ mm}/^\circ\text{C}$.**

1 Introduction

As evidence in support of global warming becomes stronger, it is apparent that the anticipated rise in sea levels may be higher than expected (Rahmstorf, 2007) and the frequency and amplitude of abrupt climate change (Martrat et al., 2004; Pall et al., 2007) may also be greater. As climate events are likely to be problematic for both ecosystems (Walther et al., 2002) and human society (Khasnis and Nettleman, 2005), any aid in prediction is crucial.

Studies of past climate events could hopefully provide useful information for exploring trigger mechanisms (Cheng, et al., 2009; Liu et al, 2013). The 8.2 ka BP event is noted to be the most pronounced abrupt climate event occurring during the whole Holocene (Alley and Ágústsson, 2005). The highest magnitude variation across the low to high latitudes makes a viable target for numerical modelings (Daley et al, 2011; Morrill et al., 2011) and may offer an insight into the sensitivity of

38 climate response in different areas (Condrón and Winsor, 2011; LeGrand and Schmidt,
39 2008). This event was firstly identified in Greenland ice cores (Alley et al., 1997),
40 showing a duration of 160-yr (Thomas et al., 2007) with a temperature drop of 3.3 ± 1.1 °C
41 in central Greenland (Kobashi et al., 2007), and is known globally (Dixit et al., 2014;
42 Morrill et al., 2013; Ljung et al., 2008; Ellwood and Gose, 2006). However, as most
43 records associated with this event mainly derived from North Atlantic and Europe
44 (Daley et al., 2011; Szeroczyńska and Zawisza, 2011; Snowball et al., 2010; Hede et
45 al., 2010; Domínguez-Villar et al., 2009; Prasad et al., 2009), the question remains as
46 to how much it influenced the East Asian monsoon area (EAMA).

47 Although some proxies from lake sediments (Yu et al., 2006; Hong et al., 2009;
48 Zheng et al., 2009; Mischke and Zhang, 2010), stalagmites (Wu et al., 2012; Cheng et
49 al., 2009; Hu et al., 2008a; Wang et al., 2005; Dykoski et al., 2005) and marine
50 sediments (Zheng et al., 2010; Ge et al., 2010) do record the 8.2 ka BP event in
51 EAMA, only Hu et al. (2008a) attempted a quantitative reconstruction of rainfall by
52 using stalagmite $\Delta\delta^{18}\text{O}$ records which indicated a decrease in precipitation during the
53 event in southwest China, an area influenced by East Asian monsoon. However, the
54 resolution of this precipitation record is approximately 100-yr and needs to be
55 improved.

56 Based on the method presented by Hu et al. (2008a), this study reconstructs a 10-yr
57 averaged annual rainfall record in southwest China during the 8.2 ka BP event by
58 comparing sub-annual (Liu et al., 2013) and 3.5-yr resolution stalagmite $\delta^{18}\text{O}$ (Cheng
59 et al., 2009) records from the same moisture transport pathway. This study further
60 addresses the sensitivity of the climate of southwest China to North Atlantic cooling
61 during the 8.2 ka BP event, providing quantitative data for simulating this global
62 event in climate system models.

63 **2 Methods**

64 **2.1 Rainfall reconstruction**

65 It has been previously discussed (Hu, et al., 2008a) that, in a monsoon area, regional
66 rainfall histories could be reconstructed by using coeval stalagmite $\delta^{18}\text{O}$ comparisons
67 between two close sites located along the same atmospheric moisture transport
68 pathway, as the difference allows the removal of secondary controls, such as moisture
69 transport and temperature on $\delta^{18}\text{O}$. Working with this premise, two published high
70 resolution stalagmite $\delta^{18}\text{O}$ sequences during the 8.2 ka BP event from Heshang cave,
71 central China (Liu et al., 2013) and Dongge cave, southwest China (Cheng et al.,
72 2009), located directly upstream in the atmospheric pathway, were investigated.

73 **2.1.1 Stalagmite $\Delta\delta^{18}\text{O}$ sequence establishment**

74 There is only one high-resolution $\delta^{18}\text{O}$ record produced by stalagmite HS4 from
75 Heshang cave (30°27'N, 110°25'E), central China, covered the 8.2 ka BP period (Liu
76 et al., 2013), with an average resolution of ~0.3-yr. However, there are two published

77 stalagmite $\delta^{18}\text{O}$ records (stalagmite DA and D4) from Dongge cave (25°17'N,
78 108°5'E), southwest China (Wang et al., 2005; Dykoski et al., 2005). Since Cheng et
79 al.(2009) re-dated DA and D4 during the 8.2 ka BP period to obtain a better controlled
80 chronology, both DA and D4 $\delta^{18}\text{O}$ records with an average resolution of ~3.5-yr and
81 ~2-yr (Cheng et al., 2009) are compared with HS4 using the approach outlined in Hu
82 et al. (2008a).

83 It may be observed that the $\delta^{18}\text{O}$ records from HS4 (Fig.1a) (Liu et al., 2013), DA
84 (Fig. 1b) and D4 (Fig.1c) (Cheng et al., 2009) show similar patterns with matching
85 peaks and troughs. Typical corresponding peaks or troughs are then marked as shown
86 by dashed lines in Fig. 1 and the chronology of DA, D4 and HS4 are so matched to
87 reduce the chronology uncertainty. It should be noted that the wiggle matching is
88 within the analytical uncertainty of the U-Th chronology. As the resolutions of HS4,
89 DA and D4 are different, all the sequences were first processed to create records of
90 equivalent annual resolution and the resultant time sequences, then used to construct a
91 10-yr moving average sequence. Two new $\delta^{18}\text{O}$ difference ($\Delta\delta^{18}\text{O}$) sequences between
92 HS4 and adjusted DA records (Fig.1d) and between HS4 and adjusted D4 records (Fig.
93 1e) were thus established.

94 Though there is a systematic offset between Fig.1d and Fig.1e, generally the
95 variations and trends of the two sequences are similar, suggesting either of the two
96 $\Delta\delta^{18}\text{O}$ sequences could be used for the following reconstruction. Since the $\delta^{18}\text{O}$
97 record from Dongge cave adopted in Hu et al.(2008a) is from DA, in this study $\Delta\delta^{18}\text{O}$
98 from Fig.1d is used for further rainfall reconstruction.

99 2.1.2 Uncertainties of $\Delta\delta^{18}\text{O}$

100 Since the $\Delta\delta^{18}\text{O}$ sequence is intending to reconstruct the regional rainfall
101 quantitatively, it is necessary to assess the uncertainties of the record. The first need to
102 be taken into consideration is the chronology uncertainty. As the maximum
103 uncertainty of DA during the 8.2 ka BP period is 94-yr (Cheng et al., 2009) and the
104 average difference between the adjusted and original DA data set is ~40-yr, the
105 robustness of the approach is tested by shifting the whole DA $\delta^{18}\text{O}$ data set 50-yr
106 young and 50-yr old respectively. The three $\Delta\delta^{18}\text{O}$ sequences are shown in Fig. 2a
107 with unchanged DA chronology (in black), shifting DA 50-yr young (in blue) and 50-
108 yr old (in red). Fig 2a demonstrates that though the shifted chronology data sets do
109 increase the uncertainty of the $\Delta\delta^{18}\text{O}$ with a maximum error of 0.76‰, the general
110 variation trends are similar, suggesting that this difference method is sufficiently
111 accurate for this study.

112 Besides the chronology uncertainty, other factors may affect the uncertainty of
113 $\Delta\delta^{18}\text{O}$. Firstly, it is from the $\delta^{18}\text{O}$ analytical uncertainties from HS4 and DA, which
114 are 0.08‰ (Liu et al. 2013) and 0.15‰ (Cheng, et al., 2009) respectively. Secondly, it
115 is from the standard deviation of the 10-yr average and the largest standard deviation
116 of $\Delta\delta^{18}\text{O}$ between DA and HS4 is 0.62‰. Also, there is an estimated uncertainty of
117 0.35‰ from the model established by Hu et al. (2008a). Taking all of these factors

118 into consideration, the final uncertainty of the $\Delta \delta^{18}\text{O}$ sequence during the 8.2 ka BP
119 period could be estimated to be $\sim 0.53\%$.

120 **2.1.3 Rainfall reconstruction**

121 Based on the $\Delta \delta^{18}\text{O}$ sequence shown in Fig. 2b, the quantitative rainfall reconstruction
122 during the 8.2 ka BP period could be built by the previous model presented by Hu et
123 al. (2008a), as the established model covering the 8.2 ka BP period. The relation
124 between $\Delta \delta^{18}\text{O}$ and rainfall ($\text{Rainfall} = 189.08 \times \Delta \delta^{18}\text{O} + 1217.4$) (Hu et al., 2008a) is
125 therefore considered suitable for this study. And the uncertainties from $\Delta \delta^{18}\text{O}$ would
126 give an uncertainty of ~ 100 mm/yr for the reconstructed rainfall record.

127 The idea of reconstructing regional rainfall between two caves by comparing two
128 spatially separated cave records along the same moisture transport pathway is to
129 presume single stalagmite $\delta^{18}\text{O}$ values from monsoon areas at least contain rainfall
130 information. For Chinese stalagmite $\delta^{18}\text{O}$ values, they are indeed influenced by
131 different types of precipitation, and as well as moisture source and its pathway, local
132 condensation and evaporation processes (Dayem et al., 2010). And a recent millennial
133 climate simulation also suggests that Chinese stalagmite $\delta^{18}\text{O}$ records could be used
134 as an indicator of intensity of the East Asian summer monsoon in terms of the
135 continental scale Asian monsoon rainfall response in the upstream regions (Liu et al.,
136 2014). As both Dongge and Heshang $\delta^{18}\text{O}$ records respond to the upstream rainfall
137 respectively, the difference of the two records should be related to the regional rainfall
138 between Dongge and Heshang cave.

139 Since on decadal scale, the relationship between $\Delta \delta^{18}\text{O}$ and rainfall records was
140 confirmed (Hu et al., 2008a), here we further access this method on inter-annual time
141 scale. Compared with local precipitation $\delta^{18}\text{O}$ ($\delta^{18}\text{O}_p$), an outside cave signal,
142 monitoring cave drip water $\delta^{18}\text{O}$ ($\delta^{18}\text{O}_d$) signals from both DA and HS4 sites should
143 reflect speleothem $\delta^{18}\text{O}$ variations more directly. Though there is no published
144 monitoring data from Dongge, there are some latest published cave monitoring $\delta^{18}\text{O}_d$
145 data between May 2011 and April 2014 with local $\delta^{18}\text{O}_p$ data (Duan et al., 2016) from
146 a cave named Liangfeng ($26^\circ 16' \text{N}$, $108^\circ 03' \text{E}$), close to Dongge ($25^\circ 17' \text{N}$, $108^\circ 5' \text{E}$),
147 which might be an alternative to assess the rainfall reconstruction method.

148 There are three separate sequences of $\delta^{18}\text{O}_d$ from different dripping sites in
149 Liangfeng cave (Zeng et al, 2015). Among them, LF6 $\delta^{18}\text{O}_d$ with a lowest drip rate
150 but highest variation amplitude has been selected, as it may record climate
151 information more efficiently. The lowest drip rate of LF6 from Liangfeng cave
152 indicates fresh water mixed with more stored water for this dripping site (Zeng et al,
153 2015), which may provide longer term instead of seasonal information compared with
154 the other two sites. Based on the 3-yr monthly monitoring data of LF6 and HS4 (Duan
155 et al., 2016), the sequences of annual moving average $\delta^{18}\text{O}_d$ of LF6 and HS4 have
156 been established respectively. Generally LF6 $\delta^{18}\text{O}_d$ values are higher than HS4 $\delta^{18}\text{O}_d$,
157 which is sensible since Heshang cave is further along the moisture transport pathway.
158 Since LF6 $\delta^{18}\text{O}_d$ is mixed by fresh and stored water, its response to the local rainfall
159 may be delayed. As there is a positive correlation ($R^2 = 0.62$) between the local annual
160 moving average $\delta^{18}\text{O}_p$ and the 2-month delayed annual moving average of LF6 $\delta^{18}\text{O}_d$,

161 it is presumed that LF6 $\delta^{18}\text{O}_d$ may be delayed by 2 months. And the same analysis on
162 $\delta^{18}\text{O}_d$ at HS4 site and $\delta^{18}\text{O}_p$ outside Heshang cave (Duan et al., 2015) reveals a
163 positive correlation ($R^2=0.71$) between the local annual moving average $\delta^{18}\text{O}_p$ and the
164 4-month delayed annual moving average of HS4 $\delta^{18}\text{O}_d$. Further analysis shows a
165 positive correlation ($R^2=0.72$) between the 2-month delayed annual moving average
166 of LF6 $\delta^{18}\text{O}_d$ and the 4-month delayed annual moving average of HS4 $\delta^{18}\text{O}_d$,
167 indicating the main factors controlled on both LF6 and HS4 $\delta^{18}\text{O}_d$ values should be
168 similar, so it is sensible to use their $\Delta\delta^{18}\text{O}_d$ records to discuss the efficiency of the
169 rainfall reconstruction method.

170 After the annual moving average $\Delta\delta^{18}\text{O}_d$ sequence between 2-month delayed LF6
171 $\delta^{18}\text{O}$ and 4-month delayed HS4 $\delta^{18}\text{O}_d$ has been built, the correlation between $\Delta\delta^{18}\text{O}_d$
172 and the regional average annual rainfall amount from six sites between Dongge cave
173 and Heshang cave mentioned in Hu et al. (2008a) could be analyzed. The regional
174 average annual rainfall amount is calculated from monthly instrumental records
175 between May 2011 and April 2014 from <http://www.wunderground.com/history/>. Fig.
176 3 shows that there is a significant positive correlation ($R^2=0.79$) between annual
177 $\Delta\delta^{18}\text{O}_d$ and regional annual rainfall amount. The significant correlation further
178 supports the idea that the stalagmite $\Delta\delta^{18}\text{O}$ between two caves located along the same
179 moisture transport pathway could reveal the regional rainfall variation, since
180 stalagmite $\delta^{18}\text{O}$ derives from the drip water $\delta^{18}\text{O}$.

181 2.2 Mg/Ca data processing

182 In addition to $\Delta\delta^{18}\text{O}$, the Mg/Ca ratio, another important rainfall proxy, is considered
183 in this paper. The Mg/Ca data set is taken from Liu et al. (2013) measured by a JEOL
184 JXA8800R Electron Microprobe at the Department of Material Sciences, Oxford,
185 along the HS4 stalagmite growth axis. The Mg/Ca data were processed to provide
186 annual resolution and a 10-yr moving average constructed in the same way as for $\delta^{18}\text{O}$.

187 3 Results

188 The 10-yr moving average $\Delta\delta^{18}\text{O}$ records between DA and HS4 is shown in Fig. 2b.
189 It is reasonable that the DA $\delta^{18}\text{O}$ values are generally higher than those of HS4 (Fig.
190 1a and Fig.1b) as Heshang Cave is located further along the moisture transport
191 pathway, which produces a systematic $\delta^{18}\text{O}$ offset. Compared with an average $\delta^{18}\text{O}$
192 difference of 1.0‰ (Hu, et al, 2008) between HS4 and DA during the whole Holocene,
193 the average $\Delta\delta^{18}\text{O}$ value during 8.2 ka BP event shown in Fig. 2b is much lower, only
194 with a value of 0.26‰.

195 It may be observed in Fig. 2b that during the central event, some of the $\Delta\delta^{18}\text{O}$
196 values are around zero or even negative, indicating much reduced moisture transport
197 during that time. While the lowest value of $\Delta\delta^{18}\text{O}$ is nearly -0.50‰ (Fig. 2b), we do
198 not expect negative $\Delta\delta^{18}\text{O}$ values. Besides the uncertainty of ~0.53‰ produced by
199 the $\Delta\delta^{18}\text{O}$ mentioned in 2.1.2, the difference in evaporation in the two caves
200 contributes to the negative $\Delta\delta^{18}\text{O}$ as well. Actually cave monitoring data do suggest

201 evaporation during the dripping and exuding processes in dry season could result in
202 heavier drip water $\delta^{18}\text{O}$ values (Zeng et al., 2015), so evaporation must result in
203 heavier stalagmite $\delta^{18}\text{O}$ values during dry period, especially in a ventilated cave.

204 Compared with Dongge , a cave consisting of branches with twists and turns, the
205 structure of Heshang cave is much simpler only with a nearly straight main passage,
206 and with a 20 m high entrance (Hu et al., 2008b). So Heshang cave is much more
207 open and ventilated than Dongge cave, and indeed it leads to an obvious heat and
208 moisture exchange between the inside and outside cave (Hu et al, 2008b). Therefore
209 on similar dry conditions, the evaporation effect in Heshang cave is much more
210 significant than in Dongge Cave, and the drier it is, the heavier HS4 $\delta^{18}\text{O}$ values
211 would be, leading to lower or even negative $\Delta\delta^{18}\text{O}$ values between DA and HS4. That
212 means less rainfall is still related to lower $\Delta\delta^{18}\text{O}$ values with the consideration of cave
213 evaporation effect. Since the 8.2 ka BP event is the driest period during the whole
214 Holocene (Hu et al., 2008), negative $\Delta\delta^{18}\text{O}$ values produced during the centre event is
215 possible.

216 From the 10-year moving average $\Delta\delta^{18}\text{O}$ between the HS4 and DA records(Fig. 2b),
217 there is a significant change in value by 1.8‰ from 1.3‰ to -0.5‰ happened in ~70
218 years at the beginning of the event. Compared with the average amplitude of $\Delta\delta^{18}\text{O}$
219 during the whole Holocene of 1.0‰ (Hu et al., 2008a), during the 8.2 ka BP period,
220 the $\Delta\delta^{18}\text{O}$ value drops greatly and the amplitude is nearly doubled.

221 Based on the $\Delta\delta^{18}\text{O}$ record shown in Fig. 2b, using the previously determined
222 relation ($\text{Rainfall}=189.08\times\Delta\delta^{18}\text{O}+1217.4$) published in Hu et al. (2008a), the rainfall
223 record in southwest China during the 8.2 ka BP period could be established as shown
224 in Fig. 2b. Besides the support for the reconstruction method by monitoring records
225 shown in 2.1.3, stalagmite Mg/Ca ratios might provide some useful information to test
226 the robustness of the reconstructed rainfall record as well.

227 Stalagmite Mg/Ca ratio is another proxy mainly controlled by local rainfall, though
228 it may show some temperature dependence, increasing slightly with temperature raise,
229 higher Mg/Ca values usually correspond to lower rainfall (Fairchild and Treble, 2009).
230 This is understood to result from CO_2 -degassing occurring earlier during water
231 movement in dry seasons as cave water seeps more slowly, thus Ca is lost from karst
232 waters by formation of calcite earlier during transport processes and before waters
233 reach the stalagmite. Such a prior-calcite-precipitation process would be expected to
234 produce higher Mg/Ca ratios (Tremaine and Froelich, 2013; Fairchild and Treble,
235 2009). Although it is hard to obtain quantitative rainfall data from Mg/Ca ratios, the
236 change of Mg/Ca may give a qualitative indication of the rainfall variability and trend.
237 Therefore the variation trend of Mg/Ca ratios could tell whether the reconstructed
238 rainfall from $\Delta\delta^{18}\text{O}$ is reliable or not.

239 The HS4 Mg/Ca sequence presented as a 10-yr moving average record during the
240 8.2 ka BP event is shown in Fig. 2c. As high Mg/Ca values are considered to indicate
241 low rainfall, the Y axis of Mg/Ca was reversed to make the comparison clearer. Both
242 the Mg/Ca ratios and the reconstructed rainfall data are presented as 10-yr moving

243 average values. Although the two data sets show slight differences, there is a general
244 inverse relationship between the two sequences giving a correlation coefficient (R^2) of
245 0.56 ($n=219$). And overall similarity could be observed between the trends of the two
246 patterns with high (low) Mg/Ca values corresponding to low (high) rainfall, which
247 suggests that the Mg/Ca results roughly support the reconstructed rainfall record as
248 well.

249 The reconstructed rainfall record (Fig. 2b) shows a **maximum decline in annual**
250 **rainfall of 350 mm/yr**, which is nearly twice that obtained from the low-resolution
251 (~100-yr) rainfall record (Hu et al., 2008a) during the same period and the lowest
252 annual rainfall in this study is lower than that from Hu et al. (2008a) by ~100 mm.
253 This is believed to be a result of the record resolution. Fig. 2b also shows that the
254 period of decreasing rainfall at the beginning of the event lasts for ~70 years, before
255 entering into an extreme dry period. During the central period of the 8.2 ka BP event,
256 the average annual rainfall is only ~1200 mm, which appears to be the driest period
257 during the whole Holocene in this area, lasting for ~50 years. **As the rainfall**
258 **calculation developed in Hu et al. (2008a) was made by averaging annual rainfall**
259 **records from 6 sites between Heshang and Dongge and the averaged annual rainfall**
260 **between 1950 and 1990 from the 6 sites is ~1380 mm, indicating the average annual**
261 **rainfall during the central 8.2 ka BP period is less than present by ~200 mm.**

262 4 Discussions

263 It has been reported that the response of the EAMA to North Atlantic cooling during
264 the 8.2 ka BP event results from atmospheric rather than oceanic processes (Liu et al.,
265 2013). It might be assumed that the high northern latitude ice-cover reinforces
266 Northern Hemisphere cooling, increasing the temperature gradient between the high
267 and low latitudes which leads to southward migration of the inter-tropical
268 convergence zone (Chiang and Bitz, 2005; Broccoli et al., 2006). This would result in
269 weakening of the East Asian Monsoon and increased aridity around. Assessment of
270 the sensitivity of southwest China climate response to North Atlantic cooling might
271 provide a clue to how North Atlantic cooling affects the EAMA.

272 Fig. 4 demonstrates three sequences of Greenland ice core $\delta^{18}\text{O}$ (Thomas et al.,
273 2007)(Fig. 4a) , a palaeo-temperature indicator (Stuiver, et al., 1995), Greenland ice
274 core $\delta^{15}\text{N}$ (Kobashi et al., 2007)(Fig.4b), a newly developed palaeo-temperature proxy
275 (Buizert et al., 2014) and the reconstructed rainfall record in southwest China during
276 the 8.2 ka BP period(Fig. 4c). The data shown in Fig. 4a are from Thomas et al. (2007)
277 with a 3-yr resolution. To allow comparison with the reconstructed rainfall records,
278 the $\delta^{18}\text{O}$ of the ice core was processed to provide a 10-yr moving average sequence.
279 The $\delta^{15}\text{N}$ data in Fig. 4b are from Kobashi et al. (2007) with a 11-yr resolution and
280 were processed similarly.

281 As low Greenland ice $\delta^{18}\text{O}$ and $\delta^{15}\text{N}$ values indicate local cooling (Thomas et al.,
282 2007; Kobashi et al., 2007), both Fig. 4a and Fig. 4b reveal similar trends of
283 decreasing temperature during the 8.2 ka BP event. The comparison between each

284 data set in Fig. 4 suggests that the decrease in rainfall in southwest China may indeed
285 be in response to Greenland cooling. Further analysis shows a slight positive
286 correlation between Greenland ice core $\delta^{18}\text{O}$ and the reconstructed rainfall with a
287 correlation coefficient (R^2) of 0.47 ($n=219$) indicating a 1‰ drop in Greenland ice
288 core $\delta^{18}\text{O}$ could lead to ~7% decrease in rainfall in southwest China. Though there is
289 not enough $\delta^{15}\text{N}$ data to reveal further correlations, it does indicate a drop of $3.3 \pm 1\text{ }^\circ\text{C}$
290 when the 8.2 ka BP event occurred (Kobashi et al., 2007). As the reconstructed annual
291 rainfall record reveals a **maximum decrease of 350 mm**, the magnitude of rainfall
292 response of southwest China to Greenland cooling during 8.2 ka BP period could be
293 assessed as $110 \pm 30\text{ mm}/^\circ\text{C}$.

294 5 Conclusions

- 295 1. Based on a comparison of two high-resolution stalagmite $\delta^{18}\text{O}$ records from
296 Dongge cave and Heshang cave along the monsoon moisture transport
297 pathway in China, a 10-yr moving average quantitative annual rainfall record
298 in southwest China is established during the 8.2 ka BP event.
- 299 2. **Significant positive correlation between drip water annual average $\delta^{18}\text{O}$**
300 **difference from two caves along the monsoon moisture transport pathway and**
301 **the regional average annual rainfall from May 2011 to April 2014 provides a**
302 **monitoring support for the reconstruction. And similar trends between the**
303 **reconstructed rainfall sequence and the stalagmite Mg/Ca ratios, another proxy**
304 **of rainfall, further increase the confidence of the quantization of the rainfall**
305 **record.**
- 306 3. The reconstructed rainfall record shows that the annual rainfall in southwest
307 China decreased sharply by ~350 mm in 70 years when the 8.2 ka BP event
308 occurred and experienced an extreme drying period lasting for ~50 years
309 during the central event. Compared with the modern instrumental records, the
310 averaged annual rainfall in southwest China during the 8.2 ka BP event is less
311 than that of present (1950 ~ 1990) by ~200 mm.
- 312 4. **The correlation analysis between the reconstructed rainfall in southwest China**
313 **and Greenland ice core $\delta^{18}\text{O}$, an indicator of temperature, suggests that the**
314 **rainfall decrease in southwest China during the 8.2 ka BP period coupled with**
315 **Greenland cooling. And a possible response rate of $110 \pm 30\text{ mm}/^\circ\text{C}$ could be**
316 **presumed by the temperature drop derived from Greenland ice core $\delta^{15}\text{N}$ and**
317 **rainfall decrease from the reconstructed record.**

318 **Acknowledgements.** This work was supported by NSFC Grants 41371216 and
319 41130207. We thank the editor and the two anonymous reviewers for their valuable
320 comments that greatly improved the manuscript.

321 References

322 Alley, R. B. and Ágústsson, A. M.: The 8k event: cause and consequences of a
323 major Holocene abrupt climate change, *Quaternary Sci. Rev.*, 24, 1123–1149, 2005.

324 Alley, R. B., Mayewski, P. A., Sowers, T., Stuiver, M., Taylor, K. C., and Clark, P. U.:
325 Holocene climatic instability: A prominent, widespread event 8200 yr ago, *Geology*,
326 25, 483–486, 1997.

327 Broccoli, A. J., Dahl, K. A., and Stouffer, R. J.: Response of the ITCZ to Northern
328 Hemisphere cooling, *Geophys. Res. Lett.*, 33, L01702, 2006.

329 Buizert, C., Gkinis, V., Severinghaus, J. P., He, F., Lecavalier, B. S., Kindler, P.,
330 Leuenberger, M., Carlson, A. E., Vinther, B., Masson-Delmotte, V., White, J. W. C.,
331 Liu, Z., Otto-Bliesner, B., and Brook, E. J.: Greenland temperature response to
332 climate forcing during the last deglaciation, *Science*, 345, 1177–1180, 2014.

333 Cheng, H., Fleitmann, D., Edwards, R. L., Wang, X., Cruz, F. W., Auler, A. S.,
334 Mangini, A., Wang, Y., Kong, X., Burns, S. J., and Matter, A.: Timing and structure
335 of the 8.2 kyr B.P. event inferred from $\delta^{18}\text{O}$ records of stalagmites from China,
336 Oman, and Brazil, *Geology*, 37, 1007–1010, 2009.

337 Chiang, J. C. H. and Bitz, C. M.: Influence of high latitude ice cover on the marine
338 Intertropical Convergence Zone, *Clim. Dynam.*, 25, 477–496, 2005.

339 Condron, A. and Winsor, P.: A subtropical fate awaited freshwater discharged from
340 glacial Lake Agassiz, *Geophys. Res. Lett.*, 38, L03705, 2011.

341 Daley, T. J., Thomas, E. R., Holmes, J. A., Street-Perrottd, F. A., Chapman, M. R.,
342 Tindall, J. C., Valdes, P. J., Loader, N. J., Marshall, J. D., Wolff, E. W.,
343 Hopley, P. J., Atkinson, T., Barberi, K. E., Fisher, E. H., Robertson, I., Hughes,
344 P. D. M., and Roberts, C. N.: The 8200 yr BP cold event in stable isotope records
345 from the North Atlantic region, *Global Planet. Change*, 79, 288–302, 2011.

346 Dayem, K. E., Molnar, P., Battisti, D. S., and Roe, G. H.: Lessons learned from
347 oxygen isotopes in modern precipitation applied to interpretation of speleothem
348 records of paleoclimate from eastern Asia, *Earth Planet. Sc. Lett.*, 295, 219–230,
349 2010.

350 Dixit, Y., Hodell, D. A., Sinhab, R., and Petrie, C. A.: Abrupt weakening of the Indian
351 summer monsoon at 8.2 kyr B.P., *Earth Planet. Sc. Lett.*, 391, 16–23, 2014.

352 Domínguez-Villar, D., Fairchild, I. J., Baker, A., Wang, X., Edwards, R. L., and Cheng,
353 H.: Oxygen isotope precipitation anomaly in the North Atlantic region during the
354 8.2 ka event, *Geology*, 37, 1095–1098, 2009.

355 Duan, W., Ruan, J., Luo, W., Li, T., Tian, L., Zeng, G., Zhang, D., Bai, Y., Li, J., Tao,
356 T., Zhang, P., Baker, A., and Tan, M.: The transfer of seasonal isotopic variability
357 between precipitation and drip water at eight caves in the monsoon regions of
358 China, *Geochim. Cosmochim. Acta*, 183: 250–266, 2016.

359 Dykoski, C. A., Edwards, R. L., Cheng, H., Yuan, D., Cai, Y., Zhang, M., Lin, Y., Qing,
360 J., An, Z., and Revenaugh, J.: A high-resolution, absolute dated Holocene and
361 deglacial Asian monsoon record from Dongge Cave, China, *Earth Planet. Sc. Lett.*,
362 233, 71–86, 2005.

363 Ellwood, B. B. and Gose, W. A.: Heinrich H1 and 8200 yr B.P. climate events
364 recorded in Hall's Cave, Texas, *Geology*, 34, 753–756, 2006.

365 Fairchild, I. J. and Treble, P. C.: Trace elements in speleothems as recorders of
366 environmental change, *Quaternary Sci. Rev.*, 28, 449–468, 2009.

367 Ge, Q., Chu, F. Y., Xue, Z., Liu, J. P., Du, Y., and Fang, Y.: Paleoenvironmental
368 records from the northern South China Sea since the Last Glacial Maximum, *Acta*
369 *Oceanol. Sin.*, 29, 46–62, 2010.

370 Hede, M. U., Rasmussen, P., Noe-Nygaard, N., Clarke, A. L., Vinebrooke, R. D., and
371 Olsen, J.: Multiproxy evidence for terrestrial and aquatic ecosystem responses
372 during the 8.2 ka cold event as recorded at Højby Sø, Denmark, *Quaternary Res.*,
373 73, 485–496, 2010.

374 Hong, Y. T., Hong, B., Lin, Q. H., Shibata, Y., Zhua, Y. X., Leng, X. T., and Wang,
375 Y.: Synchronous climate anomalies in the western North Pacific and North Atlantic
376 regions during the last 14,000 years, *Quaternary Sci. Rev.*, 28, 840–849, 2009.

377 Hu, C., Henderson, G. M., Huang, J., Xie, S., Sun, Y., and Johnson, K. R.:
378 Quantification of Holocene Asian monsoon rainfall from spatially separated cave
379 records, *Earth Planet. Sc. Lett.*, 266, 221–232, 2008a.

380 Hu, C., Henderson, G. M., Huang, J., Chen, Z., and Johnson, K. R.: Report of a three-
381 year monitoring programme at Heshang Cave, Central China, *Int. J. Speleol.*, 37 :
382 143–151, 2008b.

383 Khasnis, A. A. and Nettleman, M. D.: Global warming and infectious disease, *Arch.*
384 *Med. Res.*, 36, 689–696, 2005.

385 Kobashi, T., Severinghaus, J. P., Brook, E. J., Barnola, J. M., and Grachev, A. M.:
386 Precise timing and characterization of abrupt climate change 8200 years ago from
387 air trapped in polar ice, *Quaternary Sci. Rev.*, 26, 1212–1222, 2007.

388 LeGrande, A. N. and Schmidt, G. A.: Ensemble, water isotope-enabled, coupled
389 general circulation modeling insights into the 8.2 ka event, *Paleoceanography*, 23,
390 PA3207, 2008.

391 Liu, Y., Henderson, G. M., Hu, C., Mason, A. J., Charnley, N., Johnson, K. R., and Xie,
392 S.: Links between the East Asian monsoon and North Atlantic climate during the
393 8,200 year event, *Nat. Geosci.*, 6, 117–120, 2013.

394 Liu, Z., Wen, X., Brady, E.C., Otto-Bliesner, B., Yu, G., Lu, H., Cheng, H., Wang, Y.,
395 Zheng, W., Ding, Y., Edwards, R.L., Cheng, J., Liu, W., and Yang, H.: Chinese cave
396 records and the East Asia Summer Monsoon, *Quaternary Sci. Rev.*, 83, 115-128,
397 2014.

398 Ljung, K., Björck, S., Renssen, H., and Hammarlund, D.: South Atlantic island record
399 reveals a South Atlantic response to the 8.2 kyr event, *Clim. Past*, 4, 35–45, 2008.

400 Martrat, B., Grimalt, J. O., Lopez-Martinez, C., Cacho, I., Sierro, F. J., Flores, J. A.,
401 Zahn, R., Canals, M., Curtis, J. H., and Hodell, D. A.: Abrupt temperature changes
402 in the western Mediterranean over the past 250,000 years, *Science*, 306, 1762–1765,
403 2004.

404 Mischke, S. and Zhang, C. J.: Holocene cold events on the Tibetan Plateau, *Global*

405 Planet. Change, 72, 155–163, 2010.

406 Morrill C., Anderson, D. M., Bauer, B. A., Buckner, R., Gille, E. P., Gross, W. S.,
407 Hartman, M., and Shah, A.: Proxy benchmarks for intercomparison of 8.2 ka
408 simulations, *Clim. Past*, 9, 423–432, 2013.

409 Morrill, C., Wagner, A. J., Otto-Bliesner, B. L., and Rosenbloom, N.: Evidence for
410 significant climate impacts in monsoonal Asia at 8.2 ka from multiple proxies and
411 model simulations, *J. Earth Environ.*, 2, 426–441, 2011.

412 Pall, P., Allen, M. R., and Stone, D. A.: Testing the Clausius–Clapeyron constraint on
413 changes in extreme precipitation under CO₂ warming, *Clim. Dynam*, 28, 351–363,
414 2007.

415 Prasad, S., Witt, A., Kienel, U., Dulski, P., Bauer, E., and Yancheva, G.: The 8.2 ka
416 event: Evidence for seasonal differences and the rate of climate change in western
417 Europe, *Global Planet. Change*, 67, 218–226, 2009.

418 Rahmstorf, S.: A semi-empirical approach to projecting future sea-level rise, *Science*,
419 315, 368–370, 2007.

420 Snowball, I., Muscheler, R., Zillén, L., Sandgren, P., Stanton, T., and Ljung, K.:
421 Radiocarbon wiggle matching of Swedish lake varves reveals asynchronous climate
422 changes around the 8.2 kyr cold even, *Boreas*, 39, 720–733, 2010.

423 Stuiver, M., Grootes, P. M., and Braziunas, T. F.: The GISP2 $\delta^{18}\text{O}$ record of the past
424 16,500 years and the role of the Sun, ocean and volcanoes, *Quaternary Res.*, 44,
425 341–354, 1995.

426 Szeroczyńska, K. and Zawisza, E.: Records of the 8200 cal BP cold event reflected in
427 the composition of subfossil Cladocera in the sediments of three lakes in Poland,
428 *Quatern. Int.*, 233, 185–193, 2011.

429 Thomas, E. R., Wolff, E. W., Mulvaney, R., Steffensen, J. P., Johnsen, S. J.,
430 Arrowsmith, C., White, J. W.C., Vaughn, B., and Popp, T.: The 8.2 ka event from
431 Greenland ice cores, *Quaternary Sci. Rev.*, 26, 70–81, 2007.

432 Tremaine, D. M. and Froelich, P.N.: Speleothem trace element signatures: A
433 hydrologic geochemical study of modern cave dripwaters and farmed calcite,
434 *Geochim. Cosmochim. Acta*, 121, 522–545, 2013.

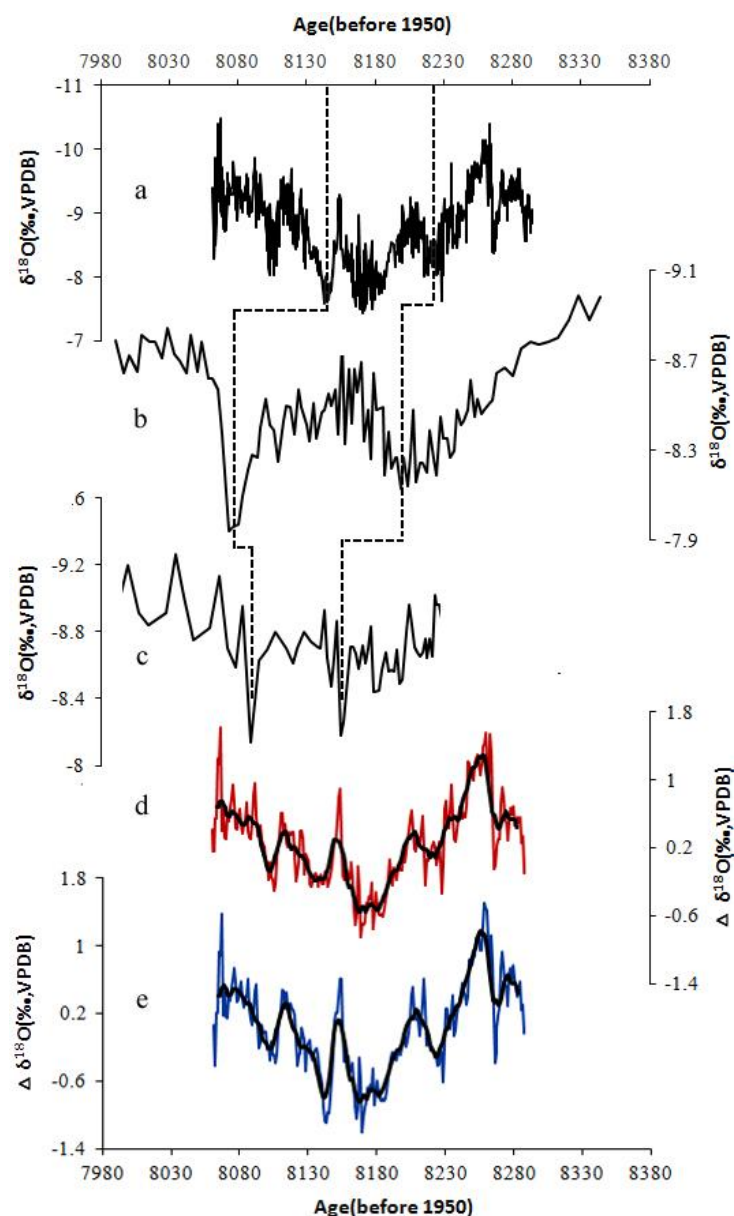
435 Walther, G. R., Post, E., Convey, P., Menzel, A., Parmesan, C., Beebee, T. J. C.,
436 Fromentin, J. M., Hoegh-Guldberg, O., and Bairlein, F.: Ecological responses to
437 recent climate change, *Nature*, 416, 389–395, 2002.

438 Wang, Y., Cheng, H., Edwards, R. L., He, Y., Kong, X., An, Z., Wu, J., Kelly, M. J.,
439 Dykoski, C. A., and Li, X.: The Holocene Asian Monsoon: links to solar changes
440 and North Atlantic climate, *Science*, 308, 854–857, 2005.

441 Wu, J., Wang, Y., Cheng, H., Kong, X., and Liu, D.: Stable isotope and trace element
442 investigation of two contemporaneous annually-laminated stalagmites from
443 northeastern China surrounding the “8.2 ka event”, *Clim. Past*, 8, 1497–1507, 2012.

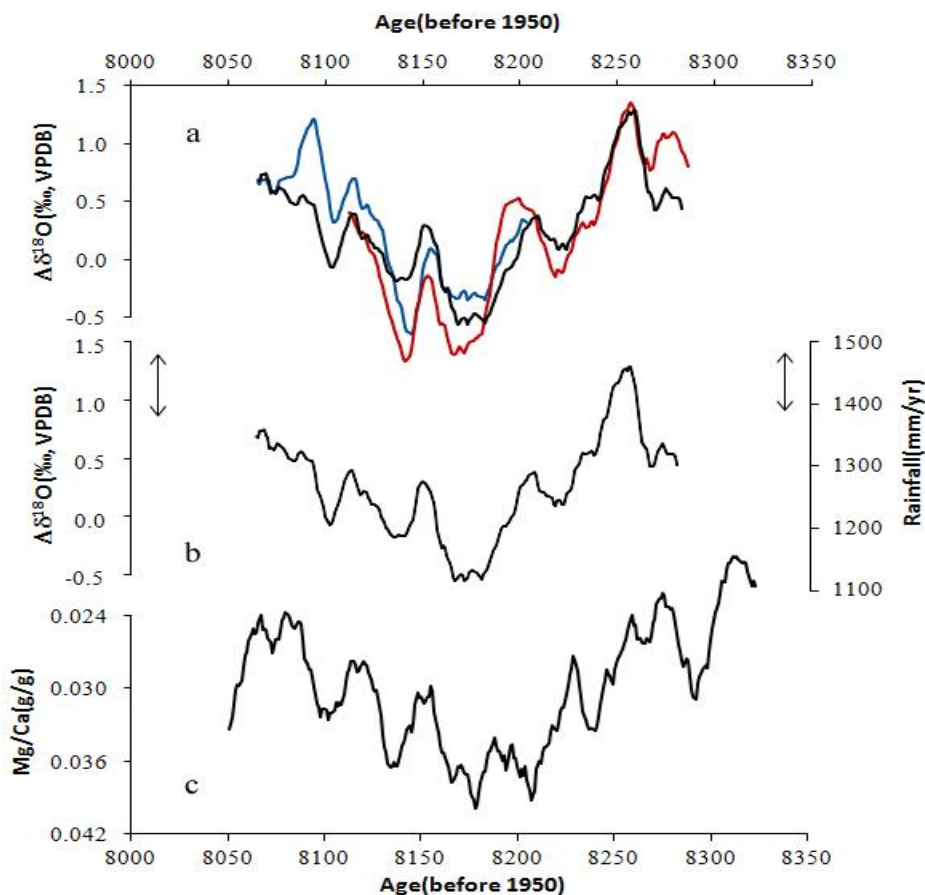
444 Yu, X., Zhou, W., Franzen, L. G., Feng, X., Peng, C., and Jull, A. J. T.: High-
445 resolution peat records for Holocene monsoon history in the eastern Tibetan Plateau,
446 *Sci. China Earth Sci.*, 49, 615–621, 2006.

447 Zeng, G., Luo, W., Wang, S., and Du, X.: Hydrogeochemical and climatic
 448 interpretations of isotopic signals from precipitation to drip waters in Liangfeng
 449 Cave, Guizhou Province, China, *Environ. Earth Sci.*,74, 1509-1519, 2015.
 450 Zheng, Y., Zhou, W., Xie, S., and Yu, X.: A comparative study of n-alkane biomarker
 451 and pollen records: an example from southern China, *Chinese Sci. Bull.*, 54, 1065–
 452 1072, 2009.
 453 Zheng, Y., Kissel, C., Zheng, H., Lajb, C., and Waang, K.: Sedimentation on the inner
 454 shelf of the East China Sea: Magnetic properties, diagenesis and paleoclimate
 455 implications, *Mar. Geol.*, 268, 34–42, 2010.
 456

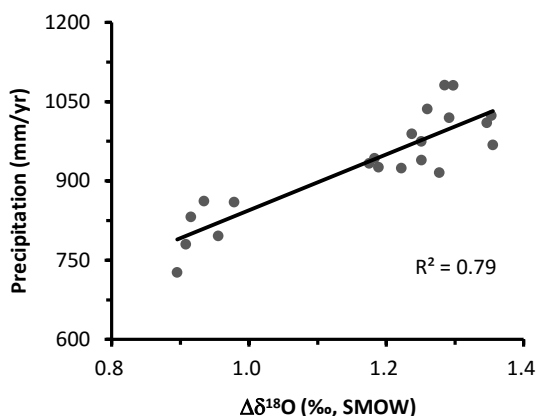


457
 458 Figure 1. Original $\delta^{18}\text{O}$ stalagmite records adopted in this paper with $\Delta\delta^{18}\text{O}$ sequences between
 459 stalagmites from Dongge and Heshang. a. HS4 $\delta^{18}\text{O}$ record from Heshang cave(Liu et al., 2013);
 460 b. DA $\delta^{18}\text{O}$ record from Dongge cave(Cheng et al., 2009); c. D4 $\delta^{18}\text{O}$ record from Dongge cave
 461 (Cheng et al., 2009); d. $\Delta\delta^{18}\text{O}$ between DA and HS4 (red) with a 10-year moving

462 average(black); e. $\Delta \delta^{18}\text{O}$ between D4 and HS4 (blue) with a 10-year moving average (black).
 463 The dashed lines show typical corresponding peaks from each original record.

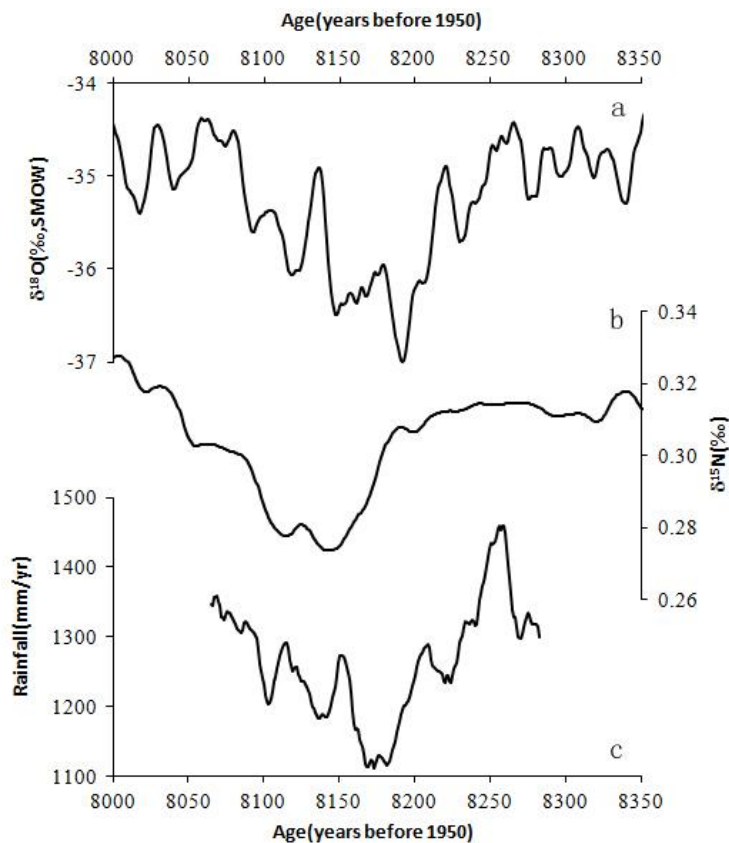


464
 465 **Figure 2.** 10-yr moving average records during the 8.2 ka BP period. a) $\Delta \delta^{18}\text{O}$ records between
 466 HS4 and DA with unchanged chronology (black), shifting DA 50-yr young (blue) and 50-yr old
 467 (red); b) $\Delta \delta^{18}\text{O}$ record between HS4 and DA and reconstructed annual rainfall in southwest
 468 China with error bars; c) Mg/Ca ratios of HS4 shown on inverted scales, which reveals a similar
 469 trend to the rainfall sequence, increasing the confidence of the quantization of the reconstructed
 470 record.



471
 472 **Figure 3.** Correlation analysis between annual moving average precipitation $\delta^{18}\text{O}$ difference
 473 of 2-month delayed LF6 and 4-month delayed HS4 from May 2011 to April 2014. The $\Delta \delta^{18}\text{O}$
 474 data are calculated from monthly monitoring data from Liangfeng cave and Heshang cave

475 (Duan et al., 2016). The annual precipitation data are the average from six sites between
476 Dongge cave and Heshang cave mentioned in Hu et al. (2008a) and the original monthly
477 rainfall data are from <http://www.wunderground.com/history/>. The correlation factor of 0.79
478 indicates a significant positive correlation between annual regional rainfall and annual $\Delta\delta^{18}\text{O}$.
479



480
481 Figure 4. Records from Greenland ice core $\delta^{18}\text{O}$ (Thomas et al., 2007) (a), Greenland ice core
482 $\delta^{15}\text{N}$ (Kobashi et al., 2007) (b) and the reconstructed annual rainfall from this study(c) during
483 the 8.2 ka BP event. Three sequences show a similar pattern indicating the decrease in rainfall
484 in southwest China coupled with Greenland cooling during the 8.2 ka BP event.
485